Boundary Load Flow Solutions

Aleksandar Dimitrovski, *Member, IEEE,* and Kevin Tomsovic, *Senior Member, IEEE*

***Abstract*—The load flow is one of the most fundamental tools used in power system analysis. The need for a load flow approach, which would incorporate uncertainty into the solution process, has been long recognized. The boundary load flow finds solutions given uncertain nodal powers. Here, a new concept for finding accurate boundary load flow solutions given fuzzy/interval numbers is presented. Extending an idea from probabilistic load flow, an optimization procedure for implicitly defined functions is introduced. Test systems are used for performance evaluation and comparison between the new method and extant methods that give approximate solutions.**

***Index Terms*—Fuzzy sets, Jacobian matrices, load flow analysis, power system planning, uncertainty.**

I. Introduction

THE load flow program is one of the most fundamental and most heavily used tools in power system analysis both for planning and operation. It provides the analyst with the steady state of the system for a specified set of load and generation values. The most common load flow approach, by far, is the deterministic load flow (DLF) where the system condition represents a snapshot in time or, more typically, a set of deterministic ("crisp") values chosen by the analyst for each input variable. This approach provides the solution for only one particular case. Often, these specified values are found by making several assumptions about the system under study, for example, future load growth patterns.

Given the fact that the uncertainty is always present under such assumptions and that one never knows the precise real conditions in the system, there is a need for numerous cases to be analyzed. In practice, analysis is repeated for under varying system conditions. The advent of deregulation and competitive power markets has increased such uncertainty even more. In this new environment, the well-known generation patterns cease to exist, the injection of power into system nodes becomes more unpredictable, and the paths of supply are more diverse.

The need for a different approach to the load flow problem, which would incorporate uncertainty into the solution process, has been long recognized. The results from such approach are expected to give solutions over the range of the uncertainties included (i.e., solutions that are sets of values instead of single points). To date, two families of such load flow algorithms have evolved.

The first, introduced in [1] and further developed over the years (for example, [2]–[6]), is the so-called probabilistic load flow (PLF). It considers load and generation as random variables with appropriate probability distributions. The results of the load flow (i.e., voltages, power flows, etc.) are also random variables with the resultant probability distributions obtained using probabilistic techniques. Because of the complexity introduced by using random variables, PLF solutions are obtained using a linearized model and the results are rough approximations.

The second family of load flow algorithms incorporating uncertainty has been developed more recently and it utilizes fuzzy sets for its modeling (for example, [7]–[9]). This is a qualitatively different way of expressing uncertainty. It represents imprecise, or vague, knowledge rather than uncertainty related to a frequency of occurrence. One inherent advantage of this approach is the ability to easily incorporate expert knowledge about the system under study. With this approach, input variables are represented as fuzzy numbers (FNs), which are special types of fuzzy sets. Although the calculations in fuzzy analysis are somewhat simpler than that in a probabilistic case (convolution is not needed), it is still far too complex to be applied directly to the full system model. Therefore, again a linearized model of the system is used and the results obtained are approximate.

In [10], an approach with interval variables is presented which uses interval methods to obtain the so-called "hull" of the solution set. This approach properly belongs to the second family since ordinary real intervals can be considered as a special case of FNs. The methodology for finding the hull of the solution set results in broad intervals that contain many nonsolution points. Such excessive uncertainty renders the results not very usable for practical purposes.

The approach proposed in this paper deals with uncertain input variables modeled as fuzzy/interval numbers. It follows the concept of a boundary load flow (BLF) presented in the context of PLF [4] and develops a methodology where an accurate solution for a nonstatistical interval load flow is obtainable from multiple ordinary "crisp" load flow solutions. Numerical results show the feasibility of this approach.

II. Foundations and Related Work

The load flow problem is given by the following two sets of nonlinear equations:

$$\mathbf{Y} = \mathbf{g}(\mathbf{X}) \qquad (1)$$

and

$$\mathbf{Z} = \mathbf{h}(\mathbf{X}) \qquad (2)$$

where

$\mathbf{X}$ vector of unknown state variables (voltage magnitudes and angles at PQ buses; and voltage angle and reactive power outputs at PV buses);

Manuscript received April 10, 2003. This work was supported in part by the National Science Foundation (NSF) under Grant DGE-0108076.

A. Dimitrovski is with the School of Electrical Engineering, University "Sv. Kiril i Metodij," Skopje, 1000, Macedonia (e-mail: aleksandar@ieee.org).

K. Tomsovic is with the School of Electrical Engineering and Computer Science, Washington State University, Pullman, WA 99164 USA (e-mail: tomsovic@eecs.wsu.edu).

Digital Object Identifier 10.1109/TPWRS.2003.821469

$\mathbf{Y}$ vector of predefined input variables (real and reactive injected nodal powers at PQ buses; and voltage magnitudes and real power outputs at PV buses);

$\mathbf{Z}$ vector of unknown output variables (real and reactive power flows in the network elements);

$\mathbf{g}, \mathbf{h}$ load flow functions.

As is well known, the major problem is the solution of the system of (1) because $\mathbf{X}$ cannot be explicitly expressed in terms of $\mathbf{Y}$ and so is instead found by an iterative process. Given a solution for $\mathbf{X}$, the solution of (2) is straightforward. In a DLF, from the initial trial solution $\mathbf{X}'$ the error is calculated as

$$\Delta\mathbf{Y} = \mathbf{Y}' - \mathbf{Y} = \mathbf{g}(\mathbf{X}') - \mathbf{Y}. \tag{3}$$

If a Newton–Raphson (N-R)-based scheme is used, (1) is linearized around $\mathbf{X}'$ and an update for the new solution is found by driving the error in (3) to zero

$$\Delta\mathbf{X} = -\mathbf{K} \cdot \Delta\mathbf{Y} \tag{4}$$

where $\mathbf{K} = \mathbf{J}_g^{-1}(\mathbf{X}')$ is the inverse Jacobian of $\mathbf{g}$ evaluated at $\mathbf{X}'$. The iteration process then continues with the new point

$$\mathbf{X}'' = \Delta\mathbf{X} + \mathbf{X}' \tag{5}$$

and the process repeats until the convergence criterion is met or the number of iterations exceeds some predefined value.

A. BLF Algorithm [4]

Within the context of PLF, this algorithm finds ranges (intervals) of values for state and output variables, given the ranges (intervals) of values of input variables from their probability distributions. The results are then used to determine multiple points of linearization for the load flow equations in order to improve the accuracy of the PLF solutions for the tail regions of probability distributions. The algorithm is presented briefly in the following.

Starting from a crisp point for input variables $\mathbf{Y}_0$ (the point of expected values), first find the deterministic solution for the state variables $\mathbf{X}_0$ that satisfies (1)

$$\mathbf{Y}_0 = \mathbf{g}(\mathbf{X}_0). \tag{6}$$

Linearizing (1) around the point $(\mathbf{X}_0, \mathbf{Y}_0)$ yields

$$\mathbf{X} = \mathbf{X}_0 + \mathbf{K} \cdot (\mathbf{Y} - \mathbf{Y}_0) \tag{7}$$

where now $\mathbf{K}$ is evaluated at $\mathbf{X}_0$. Each state variable X_i of the vector $\mathbf{X}$ is given by

$$X_t = X_{0i} + \sum_{j=1}^{m} K_{ij} \cdot (Y_j - Y_{0j}) \tag{8}$$

where m is the dimension of $\mathbf{Y}$ (and $\mathbf{X}$) and K_{ij} are elements of the sensitivity coefficient matrix $\mathbf{K}$.

The range of values for each input variable Y_j in (8) is defined and it can be represented by an interval $[Y_j^{\min}, Y_j^{\max}]$. Now suppose that the minimum value of X_i associated with this linearization is desired. The minimum value of X_i can be obtained based on the sign of K_{ij}. If K_{ij} is positive, clearly, X_i will be minimum when Y_j is minimum. Likewise, if K_{ij} is negative, X_i will be minimum when Y_j is maximum. A similar reasoning applies if the maximum value of X_i is desired.

So, for a given X_i and point of linearization $\mathbf{X}_0$, there exists a certain set of boundary values for $\mathbf{Y}$ which gives the minimum (maximum) value of X_i. Let us denote this particular $\mathbf{Y}$ with $\mathbf{Yb}_i'$. By using (7), for this $\mathbf{Yb}_i'$ we can calculate the new values of $\mathbf{X}$, $\mathbf{Xb}_i'$

$$\mathbf{Xb}_i' = \mathbf{X}_0 + \mathbf{K} \cdot \left(\mathbf{Yb}_i' - \mathbf{Y}_0\right). \tag{9}$$

The new point $(\mathbf{Xb}_i', \mathbf{Yb}_i')$, however, does not satisfy (1). Therefore, the corresponding new value $\mathbf{Yb}_i'$ must be evaluated using (1)

$$\mathbf{Yb}_i' = \mathbf{g}\left(\mathbf{Xb}_i'\right). \tag{10}$$

This process can be repeated using the new point $(\mathbf{Xb}_i', \mathbf{Yb}_i')$ as the second point of linearization with an updated value $\mathbf{Xb}_i''$ evaluated.

In the case of the output variables, $\mathbf{Z}$ a similar reasoning can be applied, provided a linear relationship between $\mathbf{Z}$ and $\mathbf{Y}$ has been established. Then linearizing both (1) and (2) around the points $(\mathbf{X}_0, \mathbf{Y}_0)$ and $(\mathbf{X}_0, \mathbf{Z}_0)$ gives

$$(\mathbf{Z} - \mathbf{Z}_0) = \mathbf{S} \cdot (\mathbf{X} - \mathbf{X}_0) = \mathbf{S} \cdot \mathbf{K} \cdot (\mathbf{Y} - \mathbf{Y}_0) \tag{11}$$

and finally

$$\mathbf{Z} = \mathbf{Z}_0 + \mathbf{L} \cdot (\mathbf{Y} - \mathbf{Y}_0) \tag{12}$$

where $\mathbf{S}$ is the Jacobian of $\mathbf{h}$ at $\mathbf{X}_0$ and $\mathbf{L} = \mathbf{S} \cdot \mathbf{K}$. The complex expressions for the elements of $\mathbf{S}$, for a general power system branch, are given in the Appendix. Equation (12) has the same form as (7) and a procedure for finding the minimum (maximum) value of some Z_i, similar to that for X_i described above, can be followed.

In some cases, some or all of the coefficients K_{ij} (L_{ij}, in the case of output variables) change their signs from iteration to iteration. This phenomenon reflects the high degree of nonlinearity associated with certain variables, especially in the case of voltage magnitudes and reactive power flows. It also presents convergence difficulties as values of $\mathbf{Y}$ oscillate from one boundary value to the other. An approach to overcome this problem, proposed in [4], is to set those input variables for which the sign of the coefficient oscillates to a fixed midpoint.

B. Fuzzy Load Flow (FLF) Algorithm [8]

When the uncertainty of input variables is of a nonstatistical nature (which the authors believe is the most usual case), FNs best represent the inputs. FNs are defined by membership functions, also known as "possibility distributions." Usually, for the sake of simplicity, trapezoidal membership functions like the one shown in Fig. 1 are assumed. A FN may also be considered as nested intervals with an α-degree of possibility, $0 \leq \alpha \leq 1$. Each α corresponds to some ordinary interval number. From this viewpoint, interval numbers and interval mathematics are simply a special case of fuzzy numbers and fuzzy mathematics. This fact is utilized when performing numerical computations with FNs. The FNs are broken down into several intervals over which computations are carried out and the resultant FN is obtained by lumping together the resultant intervals. Interval computations, in turn, consist of two or more ordinary, single point ("crisp") computations.

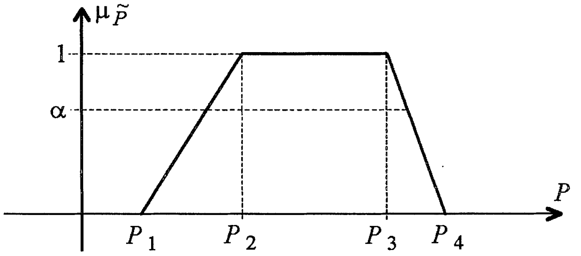

Fig. 1. Trapezoidal membership function of a fuzzy load $\tilde{P}$ expressing the possibility that load may occur between P_1 and P_4, but more typically between P_2 and P_3.

The approach presented in [8] uses linearized (7) and (12). The points of linearization $(\mathbf{X}_0, \mathbf{Y}_0)$ and $(\mathbf{X}_0, \mathbf{Z}_0)$ are obtained from a DLF with input variables set at their midpoints with the highest degree of possibility (i.e., $\alpha = 1$). These equations now have the form

$$\tilde{\mathbf{X}} = \mathbf{X}_0 + \mathbf{K} \cdot (\tilde{\mathbf{Y}} - \mathbf{Y}_0) \tag{13}$$

and

$$\tilde{\mathbf{Z}} = \mathbf{Z}_0 + \mathbf{L} \cdot (\tilde{\mathbf{Y}} - \mathbf{Y}_0) \tag{14}$$

where $\tilde{\mathbf{Y}}$ denotes the vector with fuzzy input variables, and $\tilde{\mathbf{X}}$ and $\tilde{\mathbf{Z}}$ denote the resultant vectors with fuzzy state and output variables, respectively. The sensitivity matrices $\mathbf{K}$ and $\mathbf{L}$ are "crisp" and have the same meaning as before.

Using the rules of fuzzy arithmetic [11], which are based on interval operations for a given α, the approximate resultant fuzzy variables are readily available in a few single noniterative steps. Typically, computations are performed only for two values of α ($\alpha = 0$ and $\alpha = 1$), and then assuming trapezoidal membership functions for the output variables, results for intermediary values of α are found by interpolation.

C. Monte Carlo Simulation

Monte Carlo simulation (MCS) is another feasible approach to obtaining boundary values for state and output variables. It consists of repetitive solutions of many DLFs using randomly sampled values, typically assuming a uniform distribution, for the input variables.

MCS is more appropriate for the purpose of finding an expected value than for the purpose here of finding the boundary solutions. That is, the problem is one of finding the right combination of values and there is no useful relationship between error and number of simulations as there is for determining expected values.

III. A New BLF Approach

Finding the boundary values in a load flow problem is a process of locating the constrained extrema of implicitly defined vector functions of vector arguments. In our notation, we want to find the extreme values for the elements of $\mathbf{X}$ and $\mathbf{Z}$ implicitly expressed in (1) and (2) in terms of the elements of $\mathbf{Y}$ which, in turn, are constrained.

Although the elements of $\mathbf{X}$ and $\mathbf{Z}$ cannot be explicitly expressed in terms of the elements of $\mathbf{Y}$, their partial derivatives are available. Namely, the elements K_{ij} of the sensitivity coefficient matrix $\mathbf{K}$ in (7) are actually the partial derivatives of X_i with respect to Y_j. Similarly, the elements L_{ij} of the sensitivity coefficient matrix $\mathbf{L}$ in (12) are the partial derivatives of Z_i with respect to Y_j.

Similar to derivative-based optimization procedures, by iteratively following the direction of the gradient, extreme points (possibly local) of the state or output variable can be found. Here, as in the approach from the BLF presented previously, only the signs of the partial derivatives that comprise the gradient are used. Experience has shown that the values of these partials are not useful for efficiently determining the step length. Further, a procedure is needed to maintain feasibility of the solution (i.e., ensure the input variables are within constrains for all iterations).

Suppose that the *minimum* value of X_i is sought. If K_{ij} is positive (negative), then decrease (increase) the value of Y_j. After repeating for all Y_j, using the same notation as before, we obtain a new vector of input variables $\mathbf{Y}, \mathbf{Yb}_i'$, from which a new vector of state variables $\mathbf{X}$ from (1) can be found, $\mathbf{Xb}_i'$. From this new load flow solution point $(\mathbf{Xb}_i', \mathbf{Yb}_i')$, the above steps are repeated until one of the following is true for *each* input variable:

- The partial derivative is positive and the associated variable is at a minimum.
- The partial derivative is negative and the associated variable is at a maximum;
- The partial derivative is zero.

If the final condition does not hold for any of the variables, then the solution is a vertex of the X_i's domain and clearly a point of constrained minimum. Because of the nonlinearity of the function, this point may not be the only minimum (i.e., there may be other vertices that are also points of local constrained minima). Still, our experience has shown that the physical nature of the load flow problem dictates either a unique solution or a solution, which is dominated by a few input variables in a unique manner.

When one or more of the partial derivates are zero, the solution point lies somewhere on the boundary surface. Such a point is either a local constrained extremum (either minimum or maximum) or a saddle point. Though it is highly unlikely that preceding in a downhill direction one will end up trapped in a local maximum or a saddle point, theoretically such a possibility exists. Thus, additional conditions are imposed. Previous values of X_i shall be recorded and compared with the newly obtained one. If X_i fails to decrease, then different length steps are to be employed.

Finally, in the special case when all of the partial derivatives are zero, a solution cannot be obtained due to the singularity of the Jacobian. Such a point typically indicates infeasibility of the load flow and a loading limit for the system considered. Further, a singularity of the Jacobian may occur even if not all of the partial derivatives are zero. In such cases, the ranges of values of the input variables are too great and one must repeat the calculations with reduced variations for some or all of the variables.

Based on the above discussion, a simple procedure to find the minimum value of the state variable X_i is as follows. Each input variable Y_j from $\mathbf{Y}$ is increased or decreased according to the sign of its partial derivative to the extent possible before the partial derivative changes its sign. At this point, the procedure should attempt to drive the derivative toward zero. An algorithm to achieve this is presented as pseudocode in Fig. 2.

The algorithm drives the partial derivative toward zero by embracing the input variable within an interval, which is obtained by halving the interval from the previous step. The initial interval is the predefined range of values for the input variable $[Y_j^{\min}, Y_j^{\max}]$. If at some step, a variable shows the tendency to fall outside one of the boundaries of the current interval, the boundary is reset to the initial value (either $Y_j^{\min}$ or $Y_j^{\max}$). Also, once a variable is found to lie on one of the initial boundaries, it will keep its value as long the associated partial derivative does not change sign. In the case when the maximum of X_i is sought, a simple sign change is needed to proceed. So, in the algorithm presented in Fig. 2, the parameters "up" and "down" will change to 1 and -1, respectively. When an extreme value of the output variable Z_i is sought, the procedure is identical with X_i replaced by Z_i and K_{ij} by L_{ij}.

Remarks: It should be clear that the procedure presented here, like that of [4] presented in the previous section, must be repeated for each state and output variable considered. Therefore, finding boundary values involves several load flow solutions for each variable and is computationally intensive. This is the cost of a more accurate solution than that from a linearized fuzzy/interval load flow.

After finding the new point of $\mathbf{Y}$, the new solution of the load flow is found straight from (1), instead of using (9) and then (10) for correction. Using (9) and (10) may save a few load flow iterations, but one still needs to calculate the inverse Jacobian to obtain the new $\mathbf{K}$. On the other hand, when close to the boundary solution, (10) may result in some of the variables from $\mathbf{Y}$ falling outside their predefined ranges. Those variables have to be corrected and a new solution from (1) is needed anyway.

Generally, the above algorithm works best if the first few iterations are simplified by letting the Y_j's obtain only the boundary values from their ranges (i.e., not narrowing the initial intervals to the midpoints). In this way, the process settles down before starting to chase values that diminish the partial derivatives. The proposed algorithm may occasionally fail to find the right solution if the function exhibits extreme changes during the course of solution. Still, this can be recognized by keeping track of intermediate solutions and checking the values of partial derivatives. In such cases, a warning should accompany the obtained solution.

```
up := –1; down := 1;                    % directions for minimum values
for j := 1, m                           % m – number of input variables
   Yl(j) := Ymin(j); Yh(i) := Ymax(j);  % set initial interval boundaries
   olddirection(j) := 0;                % reset directions
end for
repeat for Y, X, K                      % new solution of the load flow
  for j := 1, m
     direction(j) := sign(K(i,j));      % new direction from inverse Jacobian
     if direction(j) = up
        Yl(j) := Y(j);            % set lower bound from the current value
        if olddirection(j) = up
           Y(j) := Yh(j)          % avoid poor convergence, try boundary
           Yh(j) := Ymax(j);      % reset upper bound
        else
           Y(j) := (Yl(j)+Yh(j)) / 2;  % new value at mid interval
        end if
     else if direction(j) = down
        Yh(j) := Y(j);            % set upper bound from the current value
        if olddirection(j) = down
           Y(j) := Yl(j)          % avoid poor convergence, try boundary
           Yl(j) := Ymin(j);      % reset lower bound
        else
           Y(j) := (Yl(j)+Yh(j)) / 2;  % new value at mid interval
        end if
     end if
  end for
until abs(ΔX(i)) < tolerance
```

Fig. 2. Pseudocode of algorithm that minimizes the state variable X_i by driving the input variables Y_j, $j = 1, \ldots, m$, toward their boundary values or values where partial derivatives are zero.

IV. Convergence Improvements for N-R DLF

The N-R DLF is a natural choice for the engine behind the BLF. It provides the Jacobian required for the BLF and has good convergence characteristics. It is important for the N-R DLF to be robust, since the BLF algorithm requires load flow solutions for points that may be far from the normal operating conditions. Thus, a robust N-R DLF will not impede the BLF and allow for solutions under widely varying conditions, including a heavily stressed system.

There are various ways to improve the convergence and robustness of a N-R DLF, some of which are identified in [12]. In addition, many implementations use some undocumented heuristic procedures and programming techniques which can be described more as an art than a science. It is outside the scope of this paper to go into details on this issue. Here, we mention a simple modification of the basic N-R algorithm [13], suitable for implementation in a computationally extensive BLF that improves robustness and convergence at the cost of a small computational overhead. It can be categorized as an approach that restricts the magnitude of corrections. A similar, though more complicated and costly approach has been proposed in [14].

Define a scalar function $f(\mathbf{X})$ associated with the vector $\Delta\mathbf{Y}$ in (3), such that

$$f = \frac{1}{2} \cdot \Delta\mathbf{Y}^{\mathrm{T}} \cdot \Delta\mathbf{Y} \tag{15}$$

where $(\cdot)^{\mathrm{T}}$ denotes transposition. Now, if f is minimized, the norm of $\Delta\mathbf{Y}$ is simultaneously minimized since f is proportional to the square of the Euclidean norm of $\Delta\mathbf{Y}$. Clearly, the global minimum of f is when the norm is zero, which is the solution point of (1). The step $\Delta\mathbf{X}$ from (4) is a descent direction for f

$$\Delta f \approx \nabla f \cdot \Delta\mathbf{X} = (\Delta\mathbf{Y}^{\mathrm{T}} \cdot \mathbf{J}) \cdot (-\mathbf{J}^{-1} \cdot \Delta\mathbf{Y}) = -\Delta\mathbf{Y}^{\mathrm{T}} \cdot \Delta\mathbf{Y} < 0. \tag{16}$$

Hence, the value of f must decrease along the direction of $\Delta\mathbf{X}$ starting from the current solution. While this may not be for the full step, for some intermediary values, it must hold. So at each iteration, the full step $\Delta\mathbf{X}$ is first attempted (since a full step provides quadratic convergence in the vicinity of the solution); however, if this does not decrease f, smaller step sizes are tried until one that decreases f is found. It is possible to find the step size that decreases f the most (i.e., that minimizes f in the direction of $\Delta\mathbf{X}$), but it is usually not worth the additional computational effort. A simple strategy of successively halving the steps as needed was used here.

V. Test Results

The three existing procedures presented in Section II and the proposed approach presented in Section III are applied to several IEEE test systems. The system data and the base case descriptions can be found elsewhere (for example, [15]). The results for the 14-bus test system, shown in Fig. 3, are given in detail and with only a summary of the results for the other test systems. In several cases, we allow an extreme variation in the input variables to show the effectiveness of the algorithm.

The results from the new BLF for the boundary values of voltage magnitudes (in per unit) are presented in Table I. There are four cases of variation of values of injected nodal powers. The corresponding interval boundaries are specified in the first row of the table as a percentage of the base case values. For example, (80%–120%) means that the interval of variation of each nodal power is between 80% and 120% of its base case value. For simplicity, the same percentages of variation are assumed for each input variable.

The most general case is considered when variations are uncorrelated. This means that the power in one bus can have a value on the high boundary, while the power in some other bus can have a value on the lower boundary or in the middle of its interval of values. This is in accord with the notion of fuzziness and "possibility," dealing with uncertainties as a result of imprecision, and such uncertainties are typically uncorrelated. If correlation is assumed then there is a linear relationship between the input variables, and the BLF degenerates into a simpler set of DLFs with input variables taking their extreme values at interval boundaries.

It is also assumed that the real and reactive powers are uncorrelated. Thus, the power factors vary and take any value defined within the rectangle $[(\mathrm{P}_{\min}, Q_{\min}), (P_{\max}, Q_{\max})]$. Other definitions of load variation are possible, for example, polar rectangle $[(S_{\min}, \varphi_{\min}), S_{\max}, \varphi_{\max})]$ and that is a matter of implementation of the algorithm.

The second most left column in Table I gives the base case voltages. To the right of each boundary solution from the BLF is the number of BLF iterations (DLF solutions) required. The specified tolerance was 1.e-4, but only three decimal places are displayed here. As expected, the bigger the variation in the input variables is, the bigger the variation in the state variables. Also, the required number of BLF iterations tends to increase with the size of variation, though that is irregular and depends on the bus.

Using the values obtained from the new BLF as the standard, Table II summarizes the ranges of errors in percentage for the values of voltage magnitudes obtained from the three approaches from Section II. The MCS solutions were obtained after 20 000 simulations. In the FLF approach, rectangular membership functions were assumed so that a single interval solution was needed for each case. The points of linearization were composed from the midpoints of the specified intervals of variation.

The errors in Table II are surprisingly small even for the greatest variation of input variables. It can be seen that both the BLF from [4] and MCS produce boundary values that are very similar to the results from the new BLF, because they all use the exact model. FLF, on the other hand, uses a linearized model, which results in a slight exaggeration of the upper boundary values (positive errors for the maximal values).

Note that by using the modification to N-R DLF presented in Section IV, it was possible to find the state of the system for variations of input variables as high as 395% and voltages as low as 0.703 p.u. (bus 5). Without the modification, the highest variation that was possible was 375%, with the lowest voltage at 0.784 p.u. (bus 14). While such voltages are not meaningful in a practical sense, they are important here for finding the possible range of power flows and also to show the problem with using a dc load flow model.

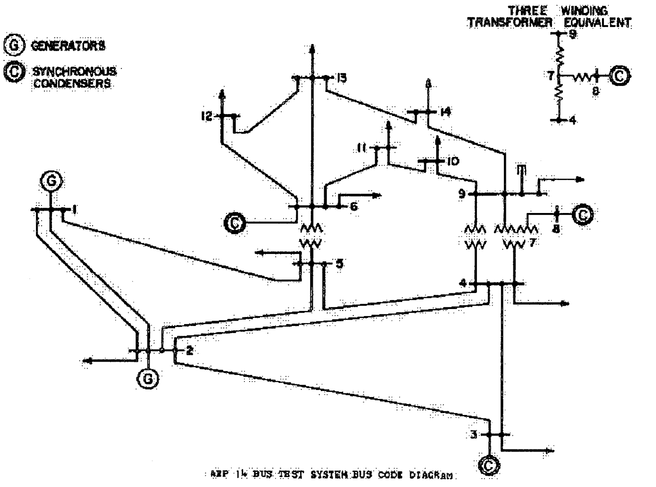
THREE WINDING TRANSFORMER EQUIVALENT
G GENERATORS
C SYNCHRONOUS CONDENSERS
1
2
3
4
5
6
7
8
9
10
11
12
13
14
AEP 14 BUS TEST SYSTEM BUS CODE DIAGRAM

Fig. 3. IEEE/AEP 14-bus test system.

Table III presents the real and reactive power flows (in per unit) using the new BLF for the same intervals of variation of injected nodal powers as before. Only a select few highly loaded and one lightly loaded branches are presented. As before, the second most left column gives the base case values and to the right of each solution from the BLF is the number of BLF iterations. The values shown are for the sending nodes (first index) of each branch.

It can be seen, as should be expected, that the variation is much larger in the flow variables. Once again, the number of BLF iterations required tends to increase with the variation, but is dependent on the particular branch. The most difficult to calculate are usually the minimal values when reverse flows occur. In such cases, the dominance of certain input variables is lost and the search for extrema is more complicated.

It is interesting to note problems with calculating the minimum value of reactive power flow Q_{1-5} when the variation of nodal powers is up to 300%. This is a case with several local minima and difficult convergence. The program issues a warning that the least value of -0.056 is one of the intermediate values found during the course of the solution, and not the converged solution which had a value -0.039. A more elaborate search method was applied to find the true minimum of -0.058. So in some extreme cases, global minima will not be found but the error appears acceptable.

Because of the wide range of values for power flows, summarizing the solutions from these approaches with only the ranges of errors may create the false impression of extremely poor results. Therefore, in Table IV, the errors (in percentage) for the boundary values of power flows for a few selected branches are given. While this table shows some extremely large errors, a closer inspection reveals that those are the errors for flows with rather small values, smaller than 0.1 p.u. where a relatively small mismatch can produce a large relative error. Usually, the small

TABLE I
BOUNDARY VALUES (IN PER UNIT) FOR THE IEEE/AEP 14-BUS SYSTEM VOLTAGE MAGNITUDES OBTAINED FROM THE NEW BLF FOR DIFFERENT VARIATIONS OF INJECTED NODAL POWERS

bus	[100%]	[80% – 120%]				[60% – 140%]				[0% – 200%]				[0% – 300%]			
voltage	V_0	$V_{\min}$	it.	$V_{\max}$	it.	$V_{\min}$	it.	$V_{\max}$	it.	$V_{\min}$	it.	$V_{\max}$	it.	$V_{\min}$	it.	$V_{\max}$	it.
V_4	1.019	1.012	2	1.025	2	1.005	2	1.030	5	0.978	2	1.045	4	0.911	2	1.046	7
V_5	1.020	1.014	2	1.026	2	1.007	2	1.031	2	0.981	2	1.042	4	0.912	2	1.044	6
V_7	1.062	1.056	2	1.068	2	1.049	2	1.074	2	1.024	2	1.089	6	0.967	2	1.090	7
V_9	1.056	1.046	2	1.066	2	1.036	3	1.075	2	1.001	3	1.101	5	0.923	8	1.103	6
V_{10}	1.051	1.041	2	1.061	2	1.031	2	1.070	2	0.997	2	1.096	5	0.923	8	1.097	6
V_{11}	1.057	1.051	2	1.063	2	1.045	2	1.068	2	1.025	2	1.084	5	0.985	3	1.084	5
V_{12}	1.055	1.052	2	1.059	2	1.048	2	1.062	2	1.036	2	1.072	2	1.014	2	1.072	4
V_{13}	1.050	1.045	2	1.056	2	1.040	2	1.060	2	1.023	2	1.074	2	0.990	2	1.075	2
V_{14}	1.036	1.024	2	1.047	2	1.012	2	1.058	2	0.972	2	1.089	5	0.887	3	1.090	6

TABLE II
RANGES OF ERRORS (%) FOR THE BOUNDARY VALUES OF VOLTAGE MAGNITUDES OBTAINED USING THE THREE METHODS FROM SECTION II. FOR DIFFERENT VARIATIONS OF INJECTED NODAL POWERS

method	[80% – 120%]		[60% – 140%]		[0% – 200%]		[0% – 300%]	
	$V_{\min}$	$V_{\max}$	$V_{\min}$	$V_{\max}$	$V_{\min}$	$V_{\max}$	$V_{\min}$	$V_{\max}$
BLF	0	0	0	0	0	0	0	-0.1 – 0
FLF	0	0	0 – 0.1	0 – 0.1	0.1 – 1.1	0.1 – 0.6	0.4 – 3.9	0.2 – 1.8
MCS	0.1 – 0.3	-0.3 – -0.1	0.2 – 0.4	-0.6 – -0.2	0.6 – 1.8	-1.3 – -0.3	1.0 – 5.0	-2.0 – -0.8

TABLE III
BOUNDARY VALUES (IN PER UNIT) FOR SOME OF THE REAL AND REACTIVE POWER FLOWS OBTAINED USING THE NEW BLF FOR DIFFERENT VARIATIONS OF INJECTED NODAL POWERS

power	[100%]	[80% – 120%]				[60% – 140%]				[0% – 200%]				[0% – 300%]			
flow	P_0	$P_{\min}$	it.	$P_{\max}$	it.	$P_{\min}$	it.	$P_{\max}$	it.	$P_{\min}$	it.	$P_{\max}$	it.	$P_{\min}$	it.	$P_{\max}$	it.
$P_{1\text{-}2}$	1.568	1.098	2	2.055	2	0.642	4	2.558	2	-0.652	6	4.194	2	-0.974	6	7.117	2
$P_{1\text{-}5}$	0.756	0.571	2	0.943	2	0.391	2	1.133	2	-0.132	5	1.722	2	-0.196	6	2.686	3
$P_{2\text{-}3}$	0.732	0.576	2	0.892	2	0.423	2	1.055	2	-0.020	4	1.571	2	-0.026	5	2.553	2
$P_{2\text{-}4}$	0.561	0.442	2	0.683	2	0.324	2	0.806	2	-0.019	2	1.189	2	-0.033	5	1.873	2
$P_{13\text{-}14}$	0.056	0.020	2	0.093	2	-0.016	2	0.130	2	-0.123	2	0.243	3	-0.180	2	0.386	3
	Q_0	$Q_{\min}$	it.	$Q_{\max}$	it.	$Q_{\min}$	it.	$Q_{\max}$	it.	$Q_{\min}$	it.	$Q_{\max}$	it.	$Q_{\min}$	it.	$Q_{\max}$	it.
$Q_{1\text{-}2}$	-0.204	-0.310	2	-0.087	2	-0.406	2	0.039	2	-0.614	2	0.470	2	-0.671	9	0.595	5
$Q_{1\text{-}5}$	0.035	0.016	2	0.056	2	-0.001	2	0.078	2	-0.045	2	0.158	2	-0.056	14	0.805	3
$Q_{2\text{-}3}$	0.036	0.022	2	0.053	2	0.014	2	0.076	2	0.011	9	0.166	2	0.011	9	0.167	2
$Q_{2\text{-}4}$	-0.023	-0.044	2	0.001	2	-0.063	4	0.026	2	-0.112	11	0.121	2	-0.136	10	0.325	2
$Q_{13\text{-}14}$	0.017	-0.001	2	0.035	2	-0.018	2	0.054	2	-0.069	6	0.113	2	-0.079	10	0.201	3

flows are not of concern and the planner concentrates on the large flows.

Due to space limitations, only excerpts are given for the larger IEEE test systems in Table V. The choice was made to show only those voltage magnitudes and real and reactive power flows that have the widest range of values for the given variation of input nodal powers, shown in the second row of the table. As before, that variation is specified with interval boundaries as a percentage of the base case values and is the same for each input variable. The values of variation shown are the biggest symmetrical values around 100% for which a feasible load flow solution still exists. It is clear that the bigger the system (and more uncertain variables), the bigger is the total combined uncertainty. Therefore, the biggest relative variation of the input variables decreases with the size of the system.

The previous conclusion suggests that one could introduce uncertainty over a selected subsystem. To illustrate this, we chose one bus of the IEEE-300 bus system and all of its adjacent buses to define a small subsystem. The rest of the system is left with the original "crisp" base case inputs. The chosen bus is bus 3 (230 kV) with its adjacent buses: bus 7003 (13.8-kV generator bus); bus 1 and bus 2 (115 kV); bus 7, bus 19, and bus 150 (230 kV); and bus 4 (345 kV). Within this area, we applied various uncertainties in the input variables in the same way as before. The results for the boundary values of the voltage magnitude of bus 3 are shown in Table VI. It can be seen that we can increase much more the level of uncertainty locally and obtain results with broader ranges than if we apply uncertainty system-wide.

The results show that the BLF from [4] gives very good results which, in cases with smaller variations, are almost identical to the new approach. However, the effort to produce solutions is similar in both approaches. Therefore, if one is interested in finding the accurate boundary values, the proposed procedure

TABLE IV
ERRORS (IN PERCENTAGE) IN BOUNDARY VALUES FOR SOME OF THE REAL AND REACTIVE POWER FLOWS OBTAINED USING THE METHODS FROM SECTION II. FOR DIFFERENT VARIATIONS OF INJECTED NODAL POWERS

power flow	[80% – 120%]						[60% – 140%]						[0% – 200%]						[0% – 300%]					
	$P_{\min}$			$P_{\max}$			$P_{\min}$			$P_{\max}$			$P_{\min}$			$P_{\max}$			$P_{\min}$			$P_{\max}$		
	BLF	FLF	MCS	BLF	FLF	MCS	BLF	FLF	MCS	BLF	FLF	MCS	BLF	FLF	MCS	BLF	FLF	MCS	BLF	FLF	MCS	BLF	FLF	MCS
$P_{1\text{-}2}$	0	-0.7	11.8	0	-0.4	-2.4	0	-4.6	35.2	0	-1.3	-7.8	-0.1	26.2	-78.8	0	-5.6	-19.5	-0.1	45.0	-72.2	0	-11.4	-20.6
$P_{1\text{-}5}$	0	-0.3	8.2	0	-0.2	-3.9	0	-1.7	21.2	0	-0.6	-9.0	-0.2	31.1	-198.0	0	-2.2	-17.3	-0.5	45.9	-156.9	0	-3.1	-15.7
$P_{2\text{-}3}$	0	-0.3	2.8	0	-0.2	-2.7	0	-1.5	8.5	0	-0.7	-4.0	0	188.4	-505.5	0	-3.2	-7.7	-0.4	372.8	-505.0	0	-6.6	-8.6
$P_{2\text{-}4}$	0	-0.2	5.9	0	-0.1	-5.5	0	-1.1	20.6	0	-0.5	-8.8	0	107.7	-839.7	0	-2.1	-15.4	-0.3	159.8	-670.4	0	-4.3	-12.7
$P_{13\text{-}14}$	0	-1.0	45.5	0	-0.2	-8.9	0	3.7	-113.7	0	-0.5	-12.1	0	2.7	-36.8	0	-1.8	-15.2	0	4.8	-39.6	0	-3.9	-18.0
	$Q_{\min}$			$Q_{\max}$			$Q_{\min}$			$Q_{\max}$			$Q_{\min}$			$Q_{\max}$			$Q_{\min}$			$Q_{\max}$		
	BLF	FLF	MCS	BLF	FLF	MCS	BLF	FLF	MCS	BLF	FLF	MCS	BLF	FLF	MCS	BLF	FLF	MCS	BLF	FLF	MCS	BLF	FLF	MCS
$Q_{1\text{-}2}$	0	1.7	-3.3	0	5.7	38.3	0	5.3	-8.9	0	-49.7	-164.4	0	24.2	-13.8	0	-24.4	-39.1	-42.4	61.8	0.0	-0.1	-47.5	-44.3
$Q_{1\text{-}5}$	0	-5.0	46.0	0	-1.4	-9.7	0	266.7	-1075.0	0	-4.5	-19.6	0	41.6	-66.4	0	-15.3	-22.0	-203.2	214.8	-67.5	0	-55.8	-39.5
$Q_{2\text{-}3}$	0	-10.3	7.6	0	-4.1	-3.7	0	-67.1	12.1	0	-11.7	-7.4	230.6	-488.9	0.0	0	-31.7	-14.5	10.2	-233.3	0.0	0	-77.2	-18.6
$Q_{2\text{-}4}$	0	2.5	-20.7	0	-240.0	-420.0	0	7.0	-25.9	0	-18.2	-56.1	-39.8	19.6	-25.1	0	-26.8	-45.1	-59.4	49.9	-33.8	0	-30.4	-26.5
$Q_{13\text{-}14}$	0	22.2	-555.6	0	-0.6	-14.5	0	4.3	-60.9	0	-1.7	-21.5	-1.2	7.2	-38.7	0	-4.9	-25.3	-12.2	13.1	-50.3	0	-7.1	-18.2

TABLE V
BOUNDARY VALUES (IN PER UNIT) FOR THE VOLTAGE MAGNITUDES AND REAL AND REACTIVE POWER FLOWS WITH THE LARGEST RANGES OF VALUES OBTAINED USING THE NEW BLF AND THE METHODS FROM SECTION II. FOR DIFFERENT IEEE TEST SYSTEMS

Test System	IEEE 57-bus		IEEE 118-bus		IEEE 300-bus	
nodal powers variation	[50% – 150%]		[60% – 140%]		[98.5% – 101.5%]	
voltage magnitude	V_{31}		V_{44}		V_{9033}	
	$V_{\min}$	$V_{\max}$	$V_{\min}$	$V_{\max}$	$V_{\min}$	$V_{\max}$
New BLF	0.703	1.045	0.873	1.007	0.838	0.944
BLF	0.703	1.044	0.873	1.003	0.838	0.936
FLF	0.808	1.065	0.942	1.027	0.907	0.958
MCS	0.866	0.985	0.959	1.002	0.924	0.937
real power flow	$P_{1\text{-}15}$		$P_{68\text{-}69}$		$P_{7049\text{-}49}$	
	$P_{\min}$	$P_{\max}$	$P_{\min}$	$P_{\max}$	$P_{\min}$	$P_{\max}$
New BLF	-1.863	6.122	-21.098	13.267	-2.319	13.829
BLF	-1.863	6.122	-21.098	13.267	-2.319	13.829
FLF	-2.350	5.330	-17.436	14.920	-3.168	12.275
MCS	-0.701	4.275	-8.131	4.475	2.890	6.496
reactive power flow	$Q_{12\text{-}16}$		$Q_{68\text{-}69}$		$Q_{7049\text{-}49}$	
	$Q_{\min}$	$Q_{\max}$	$Q_{\min}$	$Q_{\max}$	$Q_{\min}$	$Q_{\max}$
New BLF	-0.186	1.788	0.844	9.252	0.264	4.241
BLF	0.063	1.788	1.128	9.252	0.375	4.241
FLF	-0.644	0.821	0.392	1.864	0.042	0.732
MCS	-0.179	0.957	1.057	2.146	0.341	0.607

is more appropriate. Moreover, there exist examples, not necessarily limited to specific "pathological" cases, where large errors result if not using the new method.

Table IV shows that the FLF can produce good results for small to moderate variations in input variables. This is especially true for the real power flows, which exhibit less nonlinear dependence on the input variables. Together with the previous results for the voltages in Table II, it confirms the usability of this approach for fast calculations of the boundary values. Here again, in cases with greater uncertainty, the results will not be valid, especially for the reactive power flows and bus voltage magnitudes.

The errors for the MCS reveal that it is the least accurate of all the other methods. Though it may be improved by using a somewhat different sampling scheme, oriented toward the boundary values of input variables instead of uniform probability distribution, its accuracy will still be questionable. Furthermore, the issue of computational speed remains a serious concern.

TABLE VI
BOUNDARY VALUES (PER UNIT) FOR THE VOLTAGE MAGNITUDE OF BUS 3 (IEEE-300 BUS) FOR DIFFERENT VARIATIONS OF LOCAL POWERS

nodal powers variation	V_3	
	$V_{\min}$	$V_{\max}$
[98.5% – 101.5%]*	0.994	0.999
[90% – 110%]	0.995	0.998
[80% – 120%]	0.994	0.999
[70% – 130%]	0.991	1.000
[60% – 140%]	0.989	1.000
[50% – 150%]	0.986	1.001

* Applied system-wide

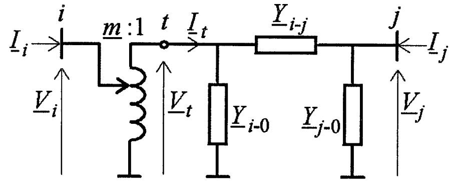

Fig. 4. General power system branch.

VI. CONCLUSION

This paper presents a new concept for finding accurate boundary values of load flow solutions. The concept is based on an optimization procedure for implicitly defined vector functions. A simple algorithm is developed that is easy to implement and performs well, in the sense that it provides a solution whenever the associated DLF converges.

Finding the accurate boundary values enables us, for the first time, to obtain accurate solutions from a fuzzy/interval load flow in which the uncertain generation and load powers are modeled with fuzzy/interval numbers. It also enables us to establish a reference for other methods that solve the same problem approximately. The results presented in the paper show that a linearized fuzzy/interval load flow can produce good results given a small degree of uncertainty very efficiently. Still, the range of validity depends on the actual system and must be verified.

Finally, when looking at boundary solutions for larger systems, one must carefully choose an appropriate level of uncertainty for each of the uncertain input variables involved. Even a small relative variation applied system-wide in an unbiased manner may render the problem infeasible. A reasonable approach is to introduce uncertainty over a particular area, or subsystem, and observe the resulting range of voltages and flows. The authors feel the developed tool can be extremely useful for planners and regulators trying to determine needed system upgrades.

Appendix
Partial Derivatives of Power Flows

Consider a general power system branch which consists of an ideal transformer with complex per unit ratio $\underline{m} : 1$ and a Π-circuit, as shown in Fig. 4. In case of a power transformer, the usual representation is an ideal transformer and serial admittance, while a transmission line is usually represented with a symmetrical Π-circuit ($\underline{m} = 1, \underline{Y}_{i-0} = \underline{Y}_{j-0}$).

The complex power flows at both nodes "i" and "j" of branch "$i - j$" are given by

$$\begin{aligned}\underline{S}_i &= P_i + jQ_i\\ &= \underline{V}_i \cdot \underline{I}_i^*\\ &= \underline{V}_i \cdot \left[\underline{V}_i \cdot \frac{(\underline{Y}_{i-0} + \underline{Y}_{i-j})}{m^2} - \underline{V}_j \cdot \frac{\underline{Y}_{i-j}}{\underline{m}^*}\right]^*\\ &= V_i^2 \cdot \frac{(\underline{Y}_{i-0} + \underline{Y}_{i-j})^*}{m^2} - \underline{V}_i \cdot \underline{V}_j^* \cdot \frac{\underline{Y}_{i-j}^*}{\underline{m}}\\ \underline{S}_j &= P_j + jQ_j\\ &= \underline{V}_j \cdot \underline{I}_j^*\\ &= \underline{V}_j \cdot \left[\underline{V}_j \cdot (\underline{Y}_{j-0} + \underline{Y}_{i-j}) - \underline{V}_i \cdot \frac{\underline{Y}_{i-j}}{\underline{m}}\right]^*\\ &= V_j^2 \cdot (\underline{Y}_{j-0} + \underline{Y}_{i-j})^* - \underline{V}_j \cdot \underline{V}_i^* \cdot \frac{\underline{Y}_{i-j}^*}{\underline{m}^*}\end{aligned}$$

where $(\cdot)^*$ denotes conjugation. The partial derivatives of the complex power flow at node "i" with respect to the magnitudes and angles of the terminal voltages are then

$$\begin{aligned}\frac{\partial \underline{S}_i}{\partial V_i} &= 2V_i \cdot \frac{(\underline{Y}_{i-0} + \underline{Y}_{i-j})^*}{m^2} - \frac{\left(\underline{V}_i \cdot \underline{V}_j^* \cdot \frac{\underline{Y}_{i-j}^*}{\underline{m}}\right)}{V_i}\\ \frac{\partial \underline{S}_i}{\partial V_j} &= \frac{-\left(\underline{V}_i \cdot \underline{V}_j^* \cdot \frac{\underline{Y}_{i-j}^*}{\underline{m}}\right)}{V_j}\\ \frac{\partial \underline{S}_i}{\partial \delta_i} &= -j\left(\underline{V}_i \cdot \underline{V}_j^* \cdot \frac{\underline{Y}_{i-j}^*}{m}\right); \quad \frac{\partial \underline{S}_i}{\partial \delta_j} = \frac{-\partial \underline{S}_i}{\partial \delta_i}.\end{aligned}$$

Similarly, the partial derivatives of the complex power flow at node "j" are

$$\begin{aligned}\frac{\partial \underline{S}_j}{\partial V_i} &= \frac{-\left(\underline{V}_j \cdot \underline{V}_i^* \cdot \frac{\underline{Y}_{i-j}^*}{\underline{m}^*}\right)}{V_i}\\ \frac{\partial \underline{S}_j}{\partial V_j} &= 2V_j \cdot (\underline{Y}_{j-0} + \underline{Y}_{i-j})^* - \frac{\left(\underline{V}_j \cdot \underline{V}_i^* \cdot \frac{\underline{Y}_{i-j}^*}{\underline{m}^*}\right)}{V_j}\\ \frac{\partial \underline{S}_j}{\partial \delta_i} &= j\left(\underline{V}_j \cdot \underline{V}_i^* \cdot \frac{\underline{Y}_{i-j}^*}{\underline{m}_*}\right); \quad \frac{\partial \underline{S}_j}{\partial \delta_j} = \frac{-\partial \underline{S}_j}{\partial \delta_i}.\end{aligned}$$

The partial derivatives of real and reactive power flows are the real and imaginary parts of the above expressions. If one is interested in the boundary values of current magnitudes, for example, because of thermal loadings, similar expressions can be derived for partial derivatives at both nodes of the corresponding elements.

References

[1] B. Borkowska, "Probabilistic load flow," *IEEE Trans. Power App. Syst.*, vol. PAS-93, pp. 752–759, May/June 1974.

[2] R. N. Allan and M. R. G. Al-Shakarchi, "Probabilistic techniques in AC load flow analysis," *Proc. Inst. Elect. Eng.*, vol. 124, no. 2, pp. 154–160, Feb. 1977.

[3] R. N. Allan, A. M. Leite da Silva, and R. C. Burchett, "Evaluation methods and accuracy in probabilistic load flow solutions," *IEEE Trans. Power App. Syst.*, vol. PAS-100, pp. 2539–2546, May 1981.

[4] R. N. Allan and A. M. Leite da Silva, "Probabilistic load flow using multilinearizations," *Proc. Inst. Elect. Eng. C*, vol. 128, no. 5, pp. 280–287, Sept. 1981.

[5] A. M. Leite da Silva and V. L. Arienti, "Probabilistic load flow by a multilinear simulation algorithm," *Proc. Inst. Elect. Eng. C*, vol. 137, no. 4, pp. 276–282, July 1990.

[6] A. P. Meliopoulos, G. J. Cokkinides, and X. Y. Chao, "A new probabilistic power analysis method," *IEEE Trans. Power Syst.*, vol. 5, pp. 182–190, Feb. 1990.

[7] V. Miranda and M. Matos, "Distribution system planning with fuzzy models and techniques," in *Proc. CIRED—10th Int. Conf. Elect. Dist.*, Brighton, U.K., 1989, pp. 472–476.

[8] V. Miranda, M. A. Matos, and J. T. Saraiva, "Fuzzy load flow—new algorithms incorporating uncertain generation and load representation," in *Proc. 10th Power Syst. Comput. Conf.*, Graz, Austria, 1990, pp. 621–627.

[9] V. Miranda and J. T. Saraiva, "Fuzzy modeling of power system optimal power flow," *IEEE Trans. Power Syst.*, vol. 7, pp. 843–849, May 1992.

[10] Z. Wang and F. L. Alvarado, "Interval arithmetic in power flow analysis," *IEEE Trans. Power Syst.*, vol. 7, pp. 1341–1349, Aug. 1992.

[11] A. Kaufmann and M. M. Gupta, *Fuzzy Mathematical Models in Engineering and Management Science*. Amsterdam, The Netherlands: Elsevier, 1988.

[12] H. W. Dommel, W. P. Tinney, and W. L. Powell, "Further developments in Newton's method for power system applications," in *Proc. IEEE Winter Power Meet.*, New York, Jan. 25–30, 1970, Paper 70CP-161-PWR.

[13] W. H. Press, S. A. Teukolsky, W. T. Wetterling, and B. P. Flannery, *Numerical Recipes in Fortran 77: The Art of Scientific Computing*, 2nd ed. Cambridge, U.K.: Cambridge Univ. Press, 1992, vol. 1, ch. 9.7.

[14] A. M. Sasson, C. Treviño, and F. Aboytes, "Improved Newton's load flow through a minimization technique," *IEEE Trans. Power App. Syst.*, vol. PAS-90, pp. 1974–1977, Sept./Oct. 1971.

[15] . [Online]http://www.ee.washington.edu/research/pstca/

Aleksandar Dimitrovski (M'95) received the B.S. and Ph.D. degrees in power engineering from University "Sv. Kiril i Metodij," Skopje, Macedonia, and the M.S. degree in application of computer sciences from the University of Zagreb, Zagreb, Croatia.

Currently, he is an Assistant Professor in power systems at University "Sv. Kiril i Metodij," on leave at Washington State University, Pullman. His research interests include advanced computing techniques in power system analysis.

Kevin Tomsovic (SM'00) received the B.S. degree in electrical engineering from Michigan Technological University, Houghton, in 1982 and the M.S. and Ph.D. degrees in electrical engineering from the University of Washington, Seattle, in 1984 and 1987, respectively.

Currently, he is a Professor at Washington State University. Visiting university positions have included Boston University, Boston, MA; National Cheng Kung University, Tainan, Taiwan, R.O.C.; National Sun Yat-Sen University, Kaohsiung, Taiwan, R.O.C.; and the Royal Institute of Technology, Stockholm, Sweden. He held the Advanced Technology for Electrical Energy Chair at Kumamoto University, Kumamoto, Japan, from 1999 to 2000.